ELEVENTH INTERNATIONAL CONFERENCE ON INTERGRANULAR AND INTERPHASE BOUNDARIES 2004

JOURNAL OF MATERIALS SCIENCE **40** (2005) 3205–3208

Simulation of martensitic microstructure

G. J. ACKLAND
School of Physics, The University of Edinburgh, Mayfield Road, Edinburgh EH9 3JZ, UK
E-mail: gjackland@ed.ac.uk

The defects appearing during the process of martensitic transformation from bcc austenite to a microtextured hcp martensite are examined, with reference to molecular dynamics simulations in zirconium. The simulations involve cooling from the high temperature austenitic bcc phase. A variety of geometric defects are identified, with the structure and dynamics being understood in terms of vicinal twin boundaries and dislocations. These defects are classified as either geometrically necessary or nanoscale effects, and the evolution of the material in response to annealing and external stress is described. The observed mechanism for twin boundary motion under applied strees involves a combination of stress concentration by preexisting sessile dislocation, causing nucleation, motion and absorption of defects in the boundary plane.

1. Introduction

When a material undergoes a martensitic transformation, the interfaces formed have very tightly-defined geometric properties and structures. The phenomenological theory of martensite [1], assumes that the transformation from austenite to martensite is diffusionless and does not result in macroscopic deformations: thus local strains are absorbed by twinning. This geometric theory contains no information about interfacial energy, and hence is scale-free.

In a phase-field model energy is associated with the strain of the material away from the perfect martensite structure. Minimisation of this energy leads to regions of perfect martensite separated by sharp twin boundaries—only at fixed boundaries does strain accrue, and this can be eliminated by forming even-finer microstructure. By contrast, with periodic boundary conditions a laminate microstructure will minimise the energy.

These geometric features are well laid out in a recent book [2], which covers most features of martensitic transitions which are independent of atomistic detail. Here we discuss the generic features which may arise in martensitic phase transitions, in particular the bcc-hcp transition observed in materials such as Zr and Ti.

An alternate approach, in which boundary energy is automatically included along with the myriad of other possible defects, is molecular dynamics. This makes no geometric assumptions about what features will exist in the final structure, beyond the information contained within the interatomic interaction potential. Thus it is possible for wholly unexpected structure to emerge. Timescales (ns) and lengthscales (submicron) for molecular dynamics simulation are typically shorter than experiment, but in the case of martensites the non-diffusional nature of the processes means that reliable pathways can be established. In this paper, we report results of such molecular dynamics simulations.

2. The BCC-HCP transition

The phase transformation from bcc to hcp is generally accepted as proceeding via a softening of the zone boundary mode T1(N) phonon mode at $(\frac{1}{2}, \frac{1}{2}, 0)$ coupled to a lattice deformation. One set of the $(110)_{\mathrm{bcc}}$ planes become the close-packed planes $(0001)_{\mathrm{hcp}}$ in the ABA stacking. Other $(110)_{\mathrm{bcc}}$ become the prism planes $(10\bar{1}0)_{\mathrm{hcp}}$.

A similar transformation can create the fcc structure (Burgers path) with the phonon at $(0, \frac{1}{3}, \frac{1}{3})$ creating an ABC stacking. More complex close packed structures may also be formed with shorter wavelength phonons. The stable close-packed structure depends on the interatomic potential used: we discuss microstructures obtained with an empirical potential fitted to zirconium, which is stable in the hcp structure with $c/a = 1.595$.

There are two features of this transformation which are atypical of the standard geometric analysis. One is the phonon coupling which leads to a doubling of the unit cell, the other is the absence of a group-subgroup relation between the austenite (bcc) and martensite (hcp). The latter occurs because the amplitude of the symmetry-breaking soft phonon and the lattice deformation take precise values to generate new symmetries in the martensite phase.

As in the geometric theory, the twinned microstructure of the molecular-dynamics-simulated martensite is constrained by the non-diffusional transition mechanism and shape conserving boundary conditions. These are automatically imposed by constant volume, periodic boundary molecular dynamics with rapid cooling. Thus the total transformation strain averaged over all twins and other defects in the cell is zero, and the

interfaces between twins are such that the close packed planes remain at the angles between $(011)_{bcc}$ planes—i.e. at 60° to the interface.

These constraints still leave a lot of freedom to the final microstructure, which typically is full of defects. To catagorise these defects, we must first define a reference structure. A convenient one is a laminate of hcp twins separated by the $(10\bar{1}1)$ symmetric twin boundary.

3. MD and analysis

The MD simulations are done using the MOLDY code [3–5] and a Finnis-Sinclair type potential which stabilises hcp zirconium at low temperature by virtue of an attraction between neighbours at (0001) [6], and bcc at high temperature through dynamic stabilisation from the entropy of soft phonons [4]. Imaging of the simulations was done by quenching a snapshot of the simulation to the nearest local energy minimum, then looking at the local environment to label each atom fcc, bcc or hcp variant 1-6. This process clearly picks out microstructural features such as the twin boundary (between hcp variants), stacking fault (strip of fcc in hcp), dislocations (line of unidentifiable atoms), etc. The definition of "local crystal structure" is somewhat arbitrary, and in highly deformed regions the assignment sometimes fails.

4. Defects associated with the phase transition

4.1. Necessary defects

The 60° twin boundary which arises from the phase transition has a vicinal structure comprising segments of the $(10\bar{1}1)$ twin with an array of dislocations to make up the misorientation (See Fig. 2). These dislocations are of basal character and are immobile in the boundary plane.

4.2. Finite size effects

4.2.1. Partial dislocations in the twin boundary

In our simulations, we find that the vicinal boundary dislocations actually correspond to partial dislocations arising from splitting of the basal dislocation with slip plane (0001); Burgers vector $\frac{1}{3}<11\bar{2}0>$. The partials reside in adjacent twin boundaries, with a stacking fault [7] running through the twin to join them. The stacking fault length is determined by the boundary separation rather than energy equilibrium: for sufficiently large twins it becomes energetically unstable with respect to a full dislocation at the boundary or one of the partials moving into the bulk [8].

These basal dislocations cannot glide in the twin boundary, however they do appear to act as stress concentrators and sources and sinks for mobile twin boundary dislocations. The diffusionless migration of twin boundaries under external strain occurs by the following process (Fig. 1):

- A mobile defect is created at a sessile partial dislocation.
- This defect moves along the boundary to an adjacent partial basal dislocation.
- The defect is absorbed by the adjacent partial basal dislocation.

This process has the net effect of advancing the twin boundary by a single pyramidal $(10\bar{1}1)$ plane in the region between the partials. The stacking fault is extended (or contracted) by one atomic spacing.

4.3. Number of variants

We consider that there are essentially six different hcp variants, which can be derived from the fact that the hcp basal plane axis can lie along any of six (110) directions. From symmetry grounds it is sometimes argued that

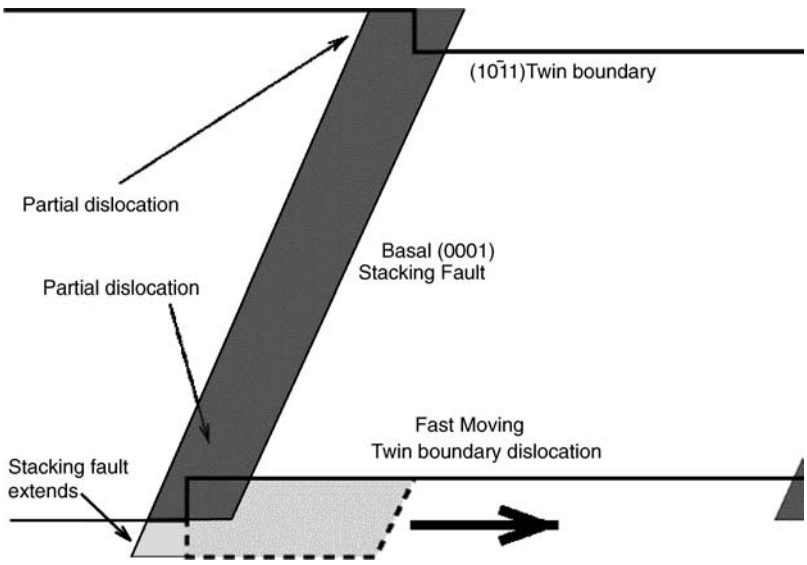

Figure 1 Schematic of the mechanism for twin boundary motion. Sessile partial dislocation (green) concentrates stress, creating unstable defect (dotted line) which glides in the twin plane until it encounters the next sessile partial. Monolayer of material coloured purple is transferred from one twin to the other as the boundary segment moves. The mechanism is similar to that observed in $(10\bar{1}2)$ twins involving crystal dislocations [10].

there are 12 variants, and from different phases of the T1(N) phonon it is possible to generate ABA and CBC stacking with the same (0001) direction, such variants being separated by a stacking fault [7], however we treat these as equivalent.

The number of variants actually observed is typically less than six. For very fast quenching the system is dominated by dynamics which leads to a combination of three variants whose interfaces share a particular $<111>_{bcc}$ direction. This is because there is little strain along the $<111>_{bcc}$ direction which transforms to $<10\bar{1}0>_{hcp}$ direction. e.g. the dynamical strain associated with the $(1\bar{1}0)_{bcc}$ planes becoming $(0001)_{hcp}$ preferentially induces a transformation in the adjoining regions of variants based on $(0\bar{1}1)_{bcc}$ and $(\bar{1}01)_{bcc}$. These three variants are sufficient to accommodate the transformation strain, so further variants are not produced (see Fig. 3). This is equivalent to a particular choice of invariant plane in the austenite/martensite transition—i.e. one close to (111).

However, it is geometrically difficult to create a microstructure with the three variants all connected by the low-energy vicinal symmetric twin boundary: typically high energy antisymmetric twins are formed. A much lower energy boundary exists between the close packed faces of $(111)_{fcc}$ and $(0001)_{hcp}$. Moreover, if the bcc $\rightarrow$ fcc transformation procedes via the Burgers mechanism then the $(1\bar{1}0)_{bcc}$, $(0\bar{1}1)_{bcc}$ and $(\bar{1}01)_{bcc}$ plane *all* transform to close packed planes in fcc. In this the fcc structure can form low energy, close packed boundaries with all three hcp variants *simultaneously*.

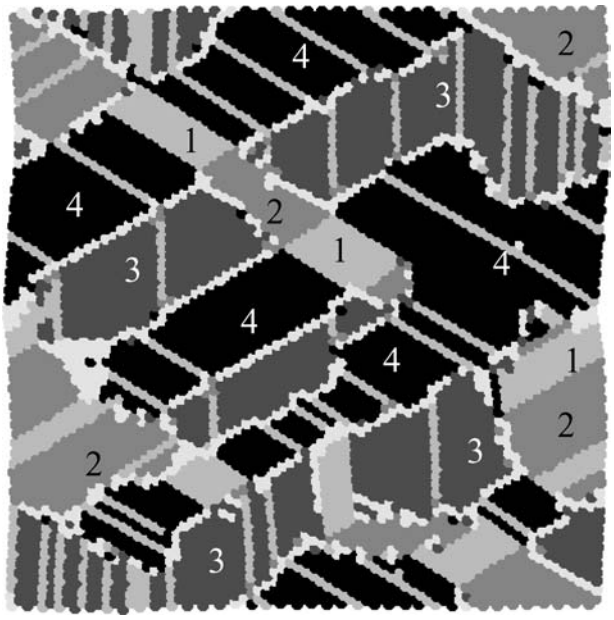

Figure 3 Image after 30ps along $(111)_{bcc}$ from rapidly quenched MD showing features of Martensitic microstructure. Light regions (labelled 1) are fcc, darker regions labelled 2-4 are three hcp variants. Light lines through the hcp variants are stacking faults, those between are atoms in the boundary. Notice that the fcc regions abut directly onto hcp regions with no "imperfect" atoms: typical stacking sequence is ...ABCABCABABABABA..., and are located in position where they could only vanish at is asymmetric twins were created. Also, contrast the sharp symmetric variant boundaries with the more diffuse asymmetric ones (the twin orientation can easily be deduced from the stacking faults each contains).

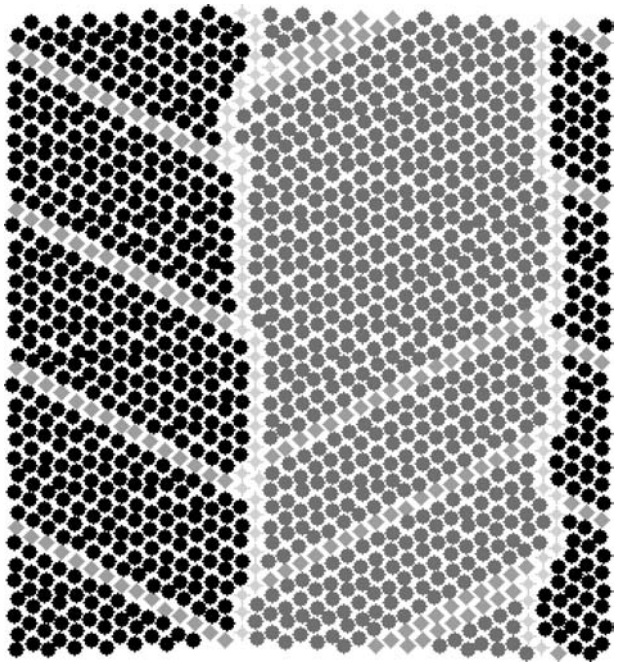

Figure 2 Image along $(111)_{bcc}$ from slow quenched MD showing features of martensitic microstructure. Circles show hcp, with variants distinguished by shading. Darker diamonds are fcc-type (i.e. stacking faults); ale diamonds represent unidentifiable atoms (i.e. the twin boundary. Two twins are evident, with boundary dislocations linked by stacking faults as discussed in the text. The image is not perfectly rectangular, since a rotation of the twins has caused a small macroscopic distortion from the original bcc structure.

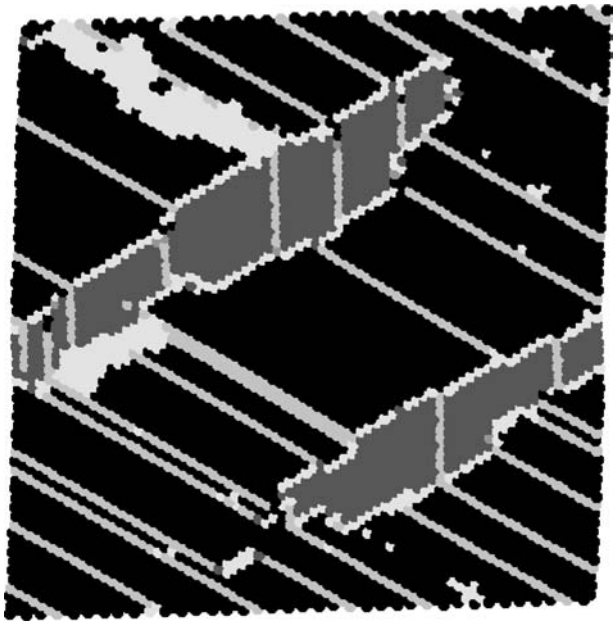

Figure 4 Later snapshot of simulation from Fig. 3 after strain has been applied to the crystal. The strain is accommodated by increasing the volume of the black variant (labelled 4 above) until only a platelike twin of variant 3 remains (periodic boundary conditions) along with two regions of plastic deformation (top left and centre left). Note that the platelike shape allows for most of the twin boundary to be vicinal, and that the tips of the variant 3 inclusion are pinned by a dislocation (evidenced by the stacking fault end). Notice that there are no free partial dislocations in the lattice—they glide freely until encountering an obstacle. Most dislocations are trapped by the twin boundary although a couple (bottom, centre) appear to have trapped one another. If the strain is further increase, the variant 3 will vanish and the dislocations will glide between self-traps of this type [5].

This leads to a feature absent in previous theories of martensite, but likely to be generic in nanoscale microstructure. Metastable phases may appear if the energy of their heterointerfaces with the stable phase is lower than the twin boundary energy. The maximum size depends on geometry and the transformation strains.

Although rapid-cooling kinetic considerations favour the production of three variants by stress-induced nucleation (Fig. 3), static relaxation can accommodate the strain with only two variants [5]. Thus on slow cooling, or after annealing, we typically find a twinned microstructure with only two variants (Fig. 2).

5. Effect of strain

External strain is applied to the material by applying a steady homogeneous deformation transformation to the atomic positions [9]. The simulated microstructure then evolves to accommodate the strain by twin boundary motion which in turn alters the relative amounts of the variants (Fig. 4). Zirconium can deform by twinning or dislocation motion, and there is some dislocation contribution from dislocations created on the annihilation of twins.

6. Conclusions

Molecular dynamics simulations have revealed a number of complicated processes occurring in the martensitic microstructure of zirconium. The well-defined twin boundaries move by a dislocation mechanism rather than diffusively. Vicinal twins tend to remain sharp, but when the geometry requires an asymmetric twin, its high energy is also manifest as a curved interface. Nanoscale effects mean that high dimensional defects (3D metastable phases and 2D stacking faults) can be stabilised by eliminating lower dimensional defects (twin boundaries, dislocations). As the microstructure coarsens, such defects vanish but may leave behind some lattice distortion.

Acknowledgements

The author would like to thank U.Pinsook for Figs 2–4. Also, Anna Serra, David Bacon and Robert Pond for discussions of the geometry of defects in the hcp crystal structure.

References

1. J. W. CHRISTIAN, "The Theory of Transformations in Metals and Alloys" (Pergamon Oxford, 1975).
2. K.BHATTACHARYA, "Microstructure of Martensite" (OUP, Oxford, 2003).
3. U. PINSOOK and G. J. ACKLAND, *Phys. Rev. B* **58** (1998) 11252.
4. *Idem.*, *ibid.* **59** (1999) 13642.
5. *Idem.*, *ibid.* **62** (2000) 5427.
6. G. J. ACKLAND, S. J. WOODING and D. J. BACON, *Philos. Mag. A* **71** (1995) 553.
7. This defect is sometimes called a hexagonal translation twin: see theory of crystal dislocations FRN nabarro (Dover, 1987) pp. 202.
8. Our simulations are too small, our stacking fault energy too low and our cooling rates too large to see this effect. However it can be readily deduced from the energy balance between dislocation strain fields and stacking fault energy.
9. Technically, changing the supercell shape while maintaining the internal coordinates.
10. R. C. POND, A. SERRA and D. J. BACON, *Acta. Materialia* **47** (1999) 1441.

Received 9 August 2004
and accepted 31 January 2005